Konya Mühendislik Bilimleri Dergisi, c. 10, s. 3, 623-633, 2022
Konya Journal of Engineering Sciences, v. 10, n. 3, 623-633, 2022
ISSN: 2667-8055 (Electronic)
DOI: 10.36306/konjes.1020246

THE INFLUENCE OF TANGENTIAL EDGE RESTRAINTS ON THE NONLINEAR RESPONSE OF LAMINATED COMPOSITE CYLINDRICAL PANELS SUBJECT TO A PINCHING FORCE

İzzet Ufuk ÇAĞDAŞ

Akdeniz University, Engineering Faculty, Civil Engineering Department, Antalya, TURKIYE
izzetufuk@akdeniz.edu.tr

Geliş/Received: 07.11.2021; Kabul/Accepted in Revised Form: 30.06.2022

ABSTRACT: In this study, the influence of straight edge tangential restraints on the nonlinear response of symmetrically laminated and balanced composite cylindrical panels subject to a pinching force is investigated. An 8-node degenerated nonlinear shell element, formulation of which is based on the Total Lagrangian Formulation, is employed for geometrically nonlinear analysis and the Arc-Length Method is used to trace the nonlinear path. First, the element is validated for geometrically non-linear analysis by solving two verification problems. Then, numerical results for different rotational boundary conditions are presented for two different stacking sequences, and thickness values. The numerical results presented show that there is no significant difference between the tangentially unrestrained and restrained clamped panels when only one edge is tangentially unrestrained. However, it is observed that the simply supported panels demonstrate a much less stiff behavior when one of the straight edges is tangentially unrestrained.

Keywords: *Laminated composite, Panel, Post-Buckling, Tangential edge Rrstraints*

Teğet Sınır Şartlarının Ortasından Tekil Yüklü Katmanlı Kompozit Silindirik Panellerin Nonlineer Davranışlarına Etkisi

ÖZET: Bu çalışmada, ortasından düşey tekil yük ile yüklü simetrik ve dengeli katmanlı kompozit silindirik panellerin nonlineer davranışlarında düz kenar teğet sınır şartlarının etkisi incelenmiştir. Bu maksatla, toplam Lagrange formulasyonuna dayanan sekiz düğümlü, dejenere ve doğrusal olmayan bir kabuk sonlu elemanı kullanılmıştır. Nonlineer davranışı gözlemleyebilmek için kiriş uzunluğu yöntemi kullanılmıştır. Öncelikle bazı doğrulama problemleri çözülerek eleman geometrik açıdan doğrusal olmayan analiz için doğrulanmıştır. Daha sonra problem farklı dönel sınır şartları, kalınlık ve katman düzenleri için incelenmiştir. Ankastre paneller için elde edilen neticeler teğet doğrultuda her iki kenar veya sadece bir kenar tutulu olduğunda davranışta önemli bir fark olmadığını göstermektedir. Ancak, basit mesnetli paneller için elde edilen neticeler rijitliğinin sadece bir kenar teğetsel doğrultuda tutulduğunda önemli nispette düştüğünü göstermektedir.

Anahtar Kelimeler: *Katmanlı kompozit, Silindirik panel, Nonlineer davranış, Teğetsel sınır şartları*

1. INTRODUCTION

In this study, the influence of straight edge tangential restraints on the nonlinear response of symmetrically laminated and balanced composite cylindrical panels subject to a pinching force is investigated. Perfect geometry is assumed and ply failure is not considered.

Almroth (1966) has examined the influence of tangential edge restrainsts on buckling of cylindrical shells in an attempt to explain the discrepancy between theory and test data. The analytical results presented by Almroth (1996) show that setting the edges free in the tangential direction results in drastic

reductions of the critical load. The influence of the tangential edge restraints on the nonlinear response and post-buckling of cylindrical shell panels has first been studied by Librescu and Lin (1997). In a more recent study, Tung (2013) has stated that the tangential constraints at the straight edges have extremely sensitive influences on the nonlinear response and postbuckling of cylindrical panels made up of functionally graded materials. The influence of tangential edge constraints on the nonlinear stability of CNT reinforced cylindrical panels has been studied by Trang and Tung (2018) and Hieu and Tung (2019). In short, it is stated in the cited studies that cylindrical panels demonstrate a highly unstable post-buckling response without the presence of tangential edge restraints. However, there are no studies in the literature on the influence of rotational boundary conditions.

Especially for shallow panels, it is of great importance to be able to predict bifurcation buckling or the snap-through buckling load. A linear stability analysis may be helpful if stability loss is of bifurcation type. However, snap-through type instability can only be determined by conducting a geometrically nonlinear analysis. The main difficulty related with nonlinear analysis is tracing the post-buckling path and to overcome this difficulty, the Arc-length Method developed by Crisfield (1981) is used in this study. However, the sign criteria proposed by Crisfield (1981) and the one by Bergan *et al*. (1978) are found out to be problematic and not reliable. Therefore, the sign criterion proposed by Neto *et al*. (2011) is selected, which includes the deformation history. A slight modification to the Arc-length Method is made here to increase the rate of convergence.

A degenerated composite shell element based on the shell element developed by Mallikarjuna and Kant (1992) is used to conduct the related structural analyses. This same element was used by Cagdas and Adali (2012(a), 2012(b)) for linearized stability analysis and design optimization of composite panels. Modification of this element for geometrically nonlinear analysis is made here by making use of the incremental total Lagrangian formulation defined by Bathe and Bolourchi (1980) and Chao and Reddy (1984). Ram and Babu (2002), Panda and Singh (2009), Bakshi and Chakravorty (2014), Singha *et al*. (2006), Barbosa and Ferreira (2009), and Sit and Ray (2019) have used similar composite shell elements for nonlinear analysis of composite panels.

First, the results obtained for two verification problems are presented and then geometrically nonlinear finite element analysis results are presented for 2 different thickness and 4 different rotational boundary conditions. Finally, the influence of tangential edge restraints on the nonlinear response is investigated.

2. THE NUMERICAL SOLUTION PROCEDURE

2.1. The Incremental Total Lagrangian Formulation

The linearized form of the equation of motion for the i^{th} iteration according to Total Lagrangian (TL) formulation is given below in Eq. (1).

$$\left\{\int_{{}^0V}\left({}^t_0\mathbf{B}_{L0}+{}^t_0\mathbf{B}_{L1}\right)^T {}_0\mathbf{C}\left({}^t_0\mathbf{B}_{L0}+{}^t_0\mathbf{B}_{L1}\right){}^0dV+\int_{{}^0V}\left({}^t_0\mathbf{B}_{NL}\right)^T\left({}^t_0\mathbf{S}\right)\left({}^t_0\mathbf{B}^T_{NL}\right)^0 dV\right\}\Delta\mathbf{u}^{(i)}=\ldots$$
$$ {}^{t+\Delta t}\mathbf{R}-\int_{{}^0V}\left({}^{t+\Delta t}_0\mathbf{B}^{(i-1)}_L\right)^T\left({}^{t+\Delta t}_0\mathbf{S}^{(i-1)}\right){}^0dV \tag{1}$$

where, the **B** matrices are the strain-displacement matrices defined by Bathe and Bolurchi (1980), ${}^t_0\mathbf{S}$ denotes the 2nd Piola-Kirchoff stresses at time t referred to the configuration at time t=0, ${}_0\mathbf{C}$ denotes the components of the elasticity tensor at time 0, **R** denotes the load vector, and the displacement increment $\Delta\mathbf{u}^{(i)}$ is defined below;

$$\Delta\mathbf{u}^{(i)}={}^{t+\Delta t}\mathbf{u}^{(i)}-{}^{t+\Delta t}\mathbf{u}^{(i-1)}. \tag{2}$$

Note that, reduced (2×2) integration is used in this study to avoid shear locking; see Pawsey and Clough (1971).

2.2. The Displacement Components

The shell element is based on the following displacement field;

$$\begin{Bmatrix} x \\ y \\ z \end{Bmatrix} = \sum_{i=1}^{nn} \begin{Bmatrix} x \\ y \\ z \end{Bmatrix}_{mid} S_i(\xi,\eta) + \frac{1}{2}\sum_{i=1}^{nn} S_i \zeta \mathbf{V}_{3i} \tag{3}$$

where, nn, $S_i(\xi,\eta)$, $\mathbf{V}_{3i}$ denote the total number of nodes, the value of the i^{th} shape function at (ξ,η) , and the unit surface normal vector at node i. The ranges of ▭and▭are -1 to 1 and the range of ▭ is $-t/2$ to $t/2$, where t denotes the thickness of the element. The nodal rotations ▭, and ▭ are shown in Fig. 1, see Cagdas and Adali (2012(a)) for details of derivation.

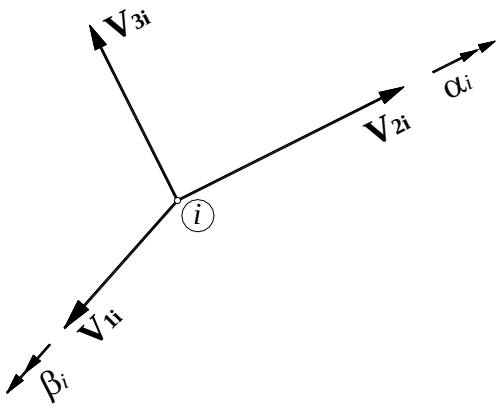

Figure 1. The global, and nodal coordinate systems

2.3. Solution of the Nonlinear Problem

The Arc-Length Method developed by Crisfield (1981) is used to solve the non-linear problem and the sign criteria proposed by Neto *et al*. (2011) is employed and a slight modification is made in the application of the Arc-Length Method. If the unbalanced loads tend to increase at a certain iteration step, then iterations are stopped to prevent divergence and the unbalanced load vector is added to the internal force vector of the next iteration. This problem may occur especially if the arc-length chosen is not suitable. This way, divergence is prevented, favorable results are obtained and it is found out that the unbalanced load diminishes rapidly.

2.4. Problem Definition

The geometry of the cylindrically curved composite panel considered in this study is shown in Fig. 2. The panel length, width, and thickness are denoted by *a*, *b*, and *t* respectively. The panels analyzed have a symmetrical stacking sequence and are constructed of six orthotropic layers of equal thickness *t*/6 and with fiber orientations θ_k where $k = 1,...,3$. The lamination angle θ is shown in Fig. 2. The panels are subject to a pinching force P and no other loads are applied. The material properties and the selected geometry

are defined in Sections 3.1 and 3.2.

The in-plane displacement components are restrained at the curved and straight edges, i.e. $u = v = w = 0$. The rotational boundary conditions of the panel are defined in Table 1. The boundary conditions considered are; SSSS: all edges simply supported, CCCC: all edges clamped, CSCS: curved edges clamped-straight edges simply supported, SCSC: curved edges simply supported-straight edges clamped. For the problem under consideration, $\mathbf{V}_{3i}$ is selected as the outward unit normal and the unit vector $\mathbf{V}_{1i}$ is calculated by multiplying $\mathbf{V}_{3i}$ with the unit vector in y direction, $\mathbf{e}_2$; i.e. $\mathbf{V}_{1i} = \mathbf{V}_{3i} \times \mathbf{e}_2$.

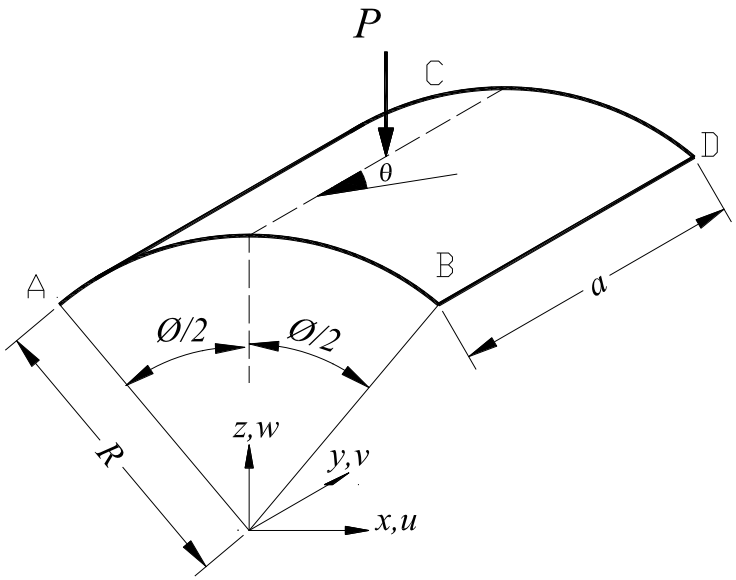

Figure 2. Cylindrical panel subject to a pinching force

Table 1. The rotational boundary conditions considered (1: free, 0: restrained)

Edge		SSSS		CCCC		SCSC		CSCS	
		α	β	α	β	α	β	α	β
curved	AB	0	1	1	0	0	1	1	0
	CD	0	1	1	0	0	1	1	0
straight	AC	1	0	0	1	0	1	1	0
	BD	1	0	0	1	0	1	1	0

3. NUMERICAL RESULTS AND DISCUSSION

First, two verification problems are solved in this section. Then, for the same geometry and material properties, the influences of the tangential and rotational edge boundary conditions on the nonlinear response are investigated. A total of 16 sample load-displacement values obtained for the boundary conditions considered are presented in Tables 2 and 3 given in the appendix. A 6x6 finite element mesh is found out to yield accurate results and therefore all of the numerical results presented are obtained using the same finite element mesh.

3.1. Verification Problems

Numerical results, obtained here using a 6x6 finite element mesh for a cylindrical panel with R=2540 mm, =0.2 rad, a=508, are compared with the numerical results presented by Sze (2004). The material properties are taken as E_{11}=3300 MPa, E_{22}=1100 MPa, G_{12}=660 MPa, =0.25 and it is assumed that

G_{13}=G_{23}=660 MPa. The curved edges are free and the straight edges are hinged. This boundary condition is named as FSFS, where letters F, and S denote "free", and "simply supported".

The numerical results obtained for t=12.7 mm and stacking sequence [90°/0°/90°] are presented in Fig. 3(a) and in Fig. 3(b) for t=6.35 mm and stacking sequence [0°/90°/0°]. It can be observed form Fig.3 that the numerical results obtained for both thickness values are in excellent agreement with the reference results.

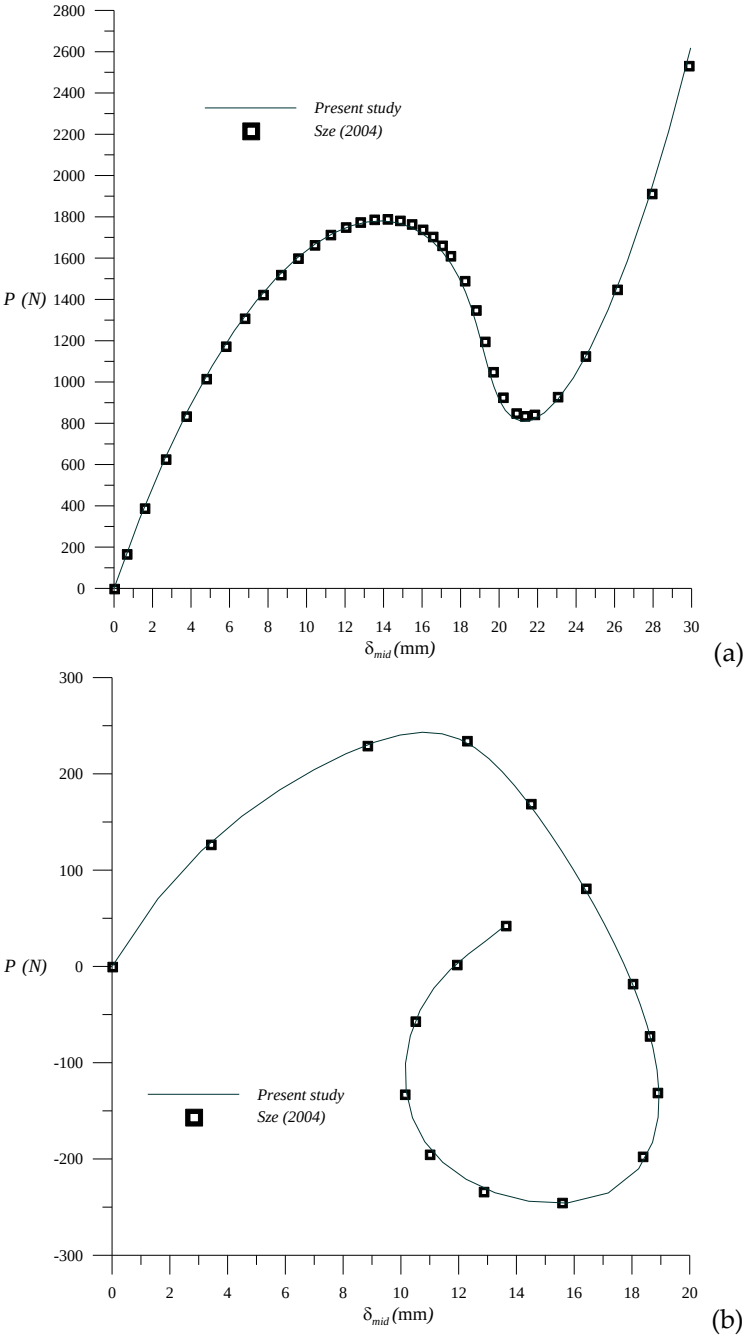

Figure 3. Load-deflection curves for FSFS cylindrical panel subject to a pinching force (a) t=12.7 mm [90°/0°/90°] (b) t=6.35 mm [0°/90°/0°]

3.2. The Influence of Rotational Boundary Conditions

Numerical results are presented in this section for the boundary conditions described in Table 1 and

the geometry, and the material properties given in Section 3.1. The following cases are considered;

Case 1: t=12.7 mm, and stacking sequence [90°/0°/90°]
Case 2: t=6.35 mm, and stacking sequence [0°/90°/0°]

The load-displacement curves for the selected cases and for all of the boundary conditions considered are presented in Fig. 4(a) and 4(b). It can be observed from Fig. 4(a) that, for Case 1, all of the boundary conditions other than FSFS B.C. yield a softening-stiffening behavior and CCCC panels are much stiffer than the SSSS panels. As expected, the nonlinear deflections for the SCSC and CSCS panels are in between the CCCC and SSSS panels, respectively. Similar deductions can be reached for t=6.35 mm panels by examining Fig. 4(b) the main difference being that the load-displacement behaviour the CSCS panel is almost identical with that of the CCCC panel. Therefore, if the straight edges are clamped, then restraining the curved edges against rotation for t=6.35 mm may not be necessary. Similary, there is no significant difference between the SSSS and SCSC panels for t=6.35 mm which implies that clamping the straight edges is not necessary if the curved edges are simply supported.

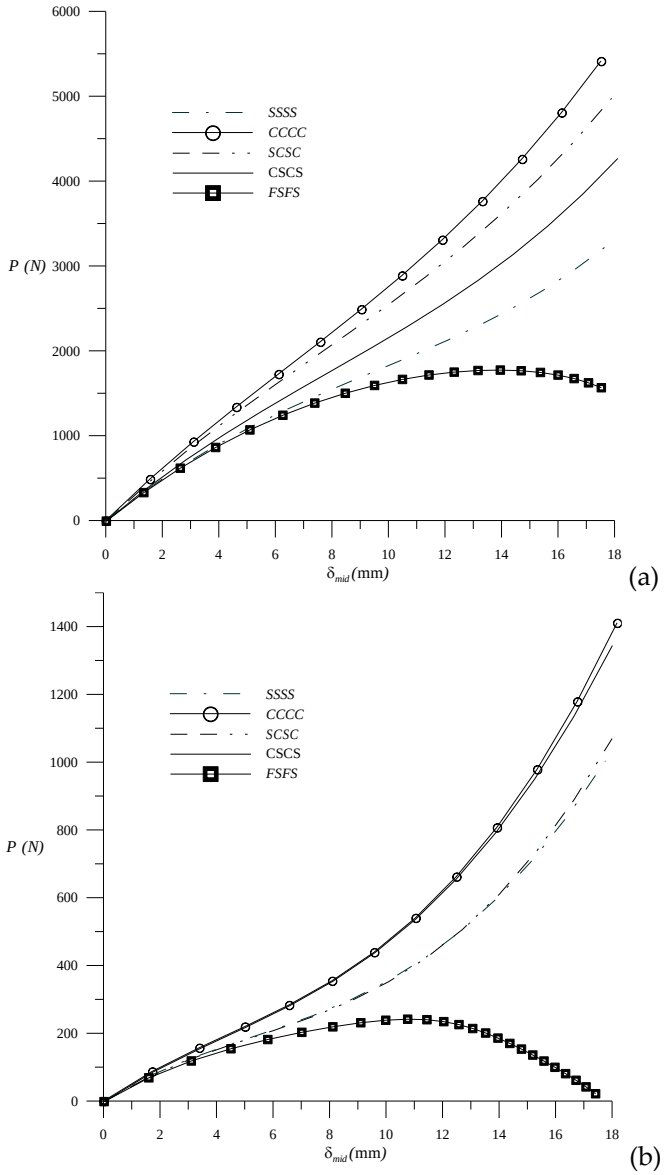

Figure 4. Load-deflection curves for the selected B.C. (a) t=12.7 mm [90°/0°/90°] (b) t=6.35 mm [0°/90°/0°]

3.3. The Influence of Tangential Edge Restraints

It's observed during this study that transforming the related dof (degrees of freedom) corresponding to the corner nodes makes the nonlinear response extremely unstable and no numerical result could be obtained for this case. Similarly, unstable nonlinear response is observed when tangential displacement is set free at both straight sides. Therefore, only one of the straight edges is set free to displace in the tangential direction and no transformation is made at the corners of the panel. The numerical results obtained are presented in Figures 5(a) and 5(b) for the "SSSS*" and "CCCC*" rotational boundary conditions respectively. The superscript "*" means that one of the straight edges of the panel is set free in the tangential direction. Comparison is also made for the FSFS B.C.

It can be observed from Figures 5(a) and 5(b) that, the results obtained for the SSSS* and CCCC* boundary conditions are very close to the results obtained for the SSSS and CCCC boundary conditions. The only difference is that, the tangentially restrained panels are slightly stiffer. Thus, it is shown that if at least one of the edges is tangentially unrestrained, the nonlinear response is stable. It can also be observed from Figures 5(a) and 5(b) that, the SSSS* panels unexpectedly have less initial stiffness comparing with the FSFS panels, which may be due to the fact that the boundary conditions are not symmetrical.

It should also be noted that the arc-length used should be selected carefully when one of the edges is unrestrained in the tangential direction as using high arc length values may cause numerical stability problems.

4. CONCLUSIONS

In this study, the influences of tangential edge restraints and rotational boundary conditions on the nonlinear response of symmetrically laminated perfect cylindrical panels subject to a pinching force are investigated.

A degenerated shell element formulation of which is based on the Total Lagrangian Formulation is used to conduct the required geometrically nonlinear analyses and the arc length method is used to trace the nonlinear path. The sign criterion proposed by Feng *et al*. (1995, 1996) is used and excellent results are obtained for the verification problems solved. It should be mentioned here that a the method is slightly modified here and if the unbalanced loads tend to increase at a certain iteration step, then iterations are stopped to prevent divergence and the unbalanced load vector is added to the internal force vector of the next iteration. This approach may be followed especially if the arc length selected is not suitable.

Then the numerical results obtained are presented. First, the nonlinear shell finite element used is verified for geometrically nonlinear analysis and then numerical results are presented for 4 different sets of rotational boundary conditions and 2 different thickness values. A softening-stiffening stable nonlinear response is observed for all of the considered rotational boundary conditions. The results also show that restraining either one of the curved or straight edges against rotation may yield the same load-displacement behavior for some panel thickness values. This means that, rotational restraints at some of the edges may not be required for some thickness values. The rotational restraint at an edge is proportional to the torsional rigidity of the stiffener and therefore, some of the stiffeners may be eliminated from design or stiffeners having low torsional rigidity may be used for some cases.

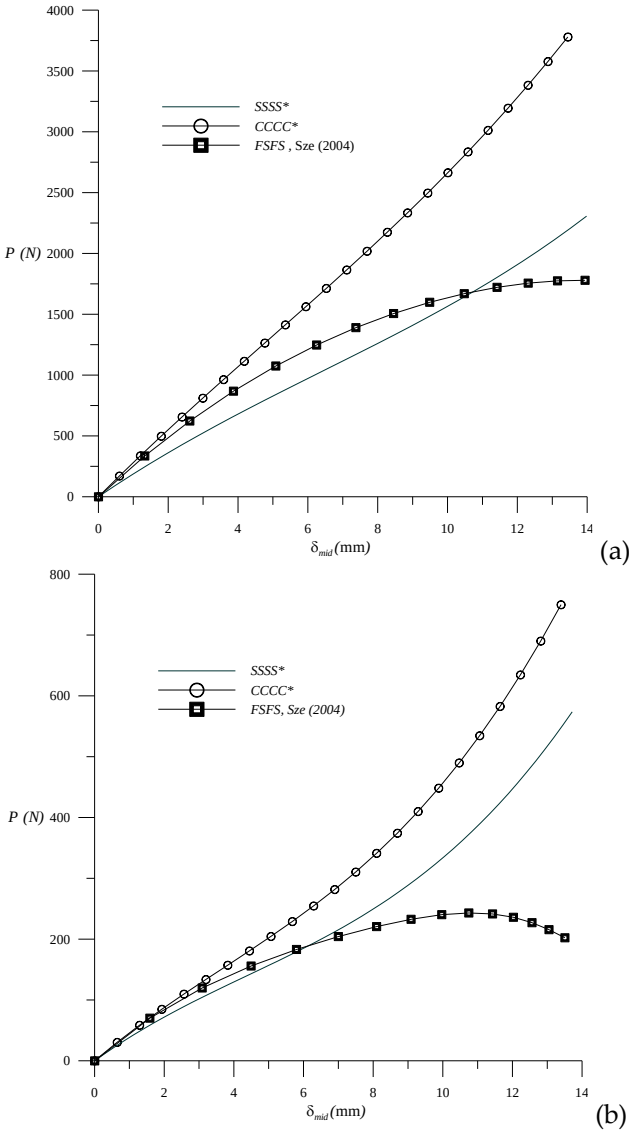

Figure 5. Load-deflection curves for SSSS* and CCCC* boundary conditions
(a) t=12.7 mm [90°/0°/90°] (b) t=6.35 mm [0°/90°/0°]

Finally, numerical results are presented for simply supported and clamped panels with one straight side tangentially unrestrained. The numerical results presented show that there is no significant difference between the tangentially unrestrained and restrained clamped panels when only one edge is tangentially unrestrained. However, it is observed that the simply supported panels demonstrate a much less stiff behavior when tangential displacements of one of the straight edges are unrestrained. It is also determined that the nonlinear response is unstable when both straight edges are tangentially unrestrained, which may cause catastrophic failure if not taken into account. A simple solution of this problem may be to use stiffeners at the straight edges, which are rigid enough to prevent failure.

Appendix

Table 2. The P (N)- δ_{mid} (mm) values obtained for Case I (t=12.7 mm, [90°/0°/90°])

SSSS		CCCC		SCSC		CSCS		SSSS*		CCCC*	
δ_{mid}	P	δ_{mid}	P	δ_{mid}	P	δ_{mid}	P	δ_{mid}	P	δ_{mid}	P
0.00	0.00	0.00	0.00	0.00	0.00	0.00	0.00	0,00	0,00	0.00	0.00
1.33	339.04	1.56	489.12	1.50	456.79	1.42	382.47	0,48	92,47	0.60	170.69
2.64	631.19	3.10	930.76	2.98	864.56	2.81	719.44	1,45	266,57	1.20	336.42
3.91	884.29	4.62	1339.01	4.43	1235.05	4.17	1020.80	2,40	428,11	1.80	497.87
5.14	1105.64	6.11	1727.07	5.85	1579.20	5.51	1295.75	3,35	579,38	2.40	655.69
6.36	1302.05	7.59	2107.22	7.25	1907.13	6.82	1552.86	4,29	722,64	3.58	963.05
7.54	1479.92	9.04	2490.84	8.63	2228.27	8.12	1800.14	5,22	860,12	4.18	1113.88
8.70	1645.32	10.48	2888.50	9.98	2551.41	9.40	2045.09	6,15	994,07	5.36	1413.04
9.85	1804.17	11.91	3310.06	11.32	2884.89	10.66	2294.88	7,08	1126,70	5.94	1562.60
10.98	1962.25	13.32	3764.79	12.65	3236.72	11.91	2556.38	8,92	1396,94	7.11	1864.69
12.09	2125.35	14.72	4261.51	13.96	3614.68	13.15	2836.31	9,84	1539,04	7.69	2018.38
13.21	2299.31	16.12	4808.69	15.27	4026.46	14.39	3141.30	10,76	1688,81	8.85	2333.86
14.32	2490.08	17.52	5414.51	16.57	4479.68	15.62	3477.99	11,68	1848,55	9.43	2496.73
15.43	2703.79	18.91	6086.95	17.87	4981.99	16.86	3853.05	12,60	2020,57	10.59	2835.33
16.55	2946.76	20.30	6833.83	19.18	5541.07	18.09	4273.23	13,52	2207,22	11.16	3012.07
17.68	3225.49	21.70	7662.88	20.49	6164.63	19.34	4745.41	14,45	2410,86	12.31	3382.79
18.82	3546.72	23.09	8581.70	21.80	6860.46	20.59	5276.58	16,32	2878,66	12.88	3577.70

Table 3. The P (N)- δ_{mid} (mm) values obtained for Case II (t=6.35 mm, [0°/90°/0°])

SSSS		CCCC		SCSC		CSCS		SSSS*		CCCC*	
δ_{mid}	P	δ_{mid}	P	δ_{mid}	P	δ_{mid}	P	δ_{mid}	P	δ_{mid}	P
0.00	0.00	0.00	0.00	0.00	0.00	0.00	0.00	0,00	0,00	0,00	0,00
1.61	73.44	1.72	87.45	1.60	73.51	1.73	87.29	0,28	11,48	0,65	30,37
3.15	127.63	3.39	157.33	3.14	127.95	3.40	156.87	0,57	22,45	1,29	58,47
4.63	171.13	5.00	219.85	4.61	171.35	5.02	219.46	1,69	61,99	2,57	109,67
6.04	210.85	6.57	283.52	6.02	210.50	6.58	283.50	2,80	96,09	3,20	133,67
7.41	252.01	8.09	354.95	7.40	250.93	8.10	355.18	3,90	126,89	4,45	180,66
8.75	298.60	9.58	439.29	8.74	297.19	9.58	438.94	4,99	156,48	5,06	204,48
10.06	353.85	11.04	540.64	10.06	353.17	11.03	538.12	6,06	186,80	6,29	254,63
11.35	420.51	12.49	662.41	11.37	422.33	12.45	655.35	7,13	219,65	6,90	281,65
12.64	501.01	13.92	807.63	12.68	507.81	13.86	792.84	8,19	256,64	8,10	341,19
13.92	597.55	15.35	979.07	13.99	612.62	15.25	952.55	9,25	299,24	8,70	374,27
15.20	712.21	16.76	1179.38	15.31	739.62	16.62	1136.28	10,31	348,82	9,88	448,32
16.48	846.97	18.18	1411.16	16.64	891.60	17.99	1345.82	11,36	406,69	10,47	489,78
17.76	1003.77	19.59	1677.02	17.98	1071.33	19.35	1583.01	12,40	474,11	11,64	582,65
19.05	1184.56	21.00	1979.63	19.32	1281.60	20.70	1849.79	13,45	552,33	12,23	634,47
20.33	1391.42	22.41	2321.76	20.68	1525.22	22.05	2148.37	14,51	642,59	13,40	749,83
21.62	1626.60	23.82	2706.29	22.04	1805.11	23.39	2481.27	15,56	746,13	13,98	813,74

REFERENCES

Almroth, B. O. (1966). Influence of edge conditions on the stability of axially compressed cylindrical shells. AIAA Journal, 4(1), 134-140.

Bakshi, K., & Chakravorty, D. (2014). Geometrically linear and nonlinear first-ply failure loads of composite cylindrical shells. Journal of Engineering Mechanics, 140(12), 04014094.

Barbosa, J. A. T., & Ferreira, A. J. M. (2009). Geometrically nonlinear analysis of functionally graded plates and shells. Mechanics of Advanced Materials and Structures, 17(1), 40-48.

Bathe, K. J., & Bolourchi, S. (1979). Large displacement analysis of three-dimensional beam structures. International journal for numerical methods in engineering, 14(7), 961-986.

Bathe, K. J., & Bolourchi, S. (1980). A geometric and material nonlinear plate and shell element. Computers & structures, 11(1-2), 23-48.

Bergan, P. G., Horrigmoe, G., Bråkeland, B., & Søreide, T. H. (1978). Solution techniques for non− linear finite element problems. International Journal for Numerical Methods in Engineering, 12(11), 1677-1696.

Cagdas, I. U., & Adali, S. (2012-b). Effect of Fiber Orientation on Buckling and First-Ply Failures of Cylindrical Shear-Deformable Laminates. Journal of Engineering Mechanics, 139(8), 967-978.

Cagdas, I., & Adali, S. (2012-a). Design of a laminated composite variable curvature panel under uniaxial compression. Engineering Computations: International Journal for Computer-Aided Engineering and Software, 29(1), 48-64.

Chao, W. C., & Reddy, J. N. (1984). Analysis of laminated composite shells using a degenerated 3-D element. International Journal for Numerical Methods in Engineering, 20(11), 1991-2007.

Crisfield, M. A. (1981). A fast incremental/iterative solution procedure that handles "snap-through". In Computational Methods in Nonlinear Structural and Solid Mechanics (pp. 55-62). Pergamon.

de Souza Neto, E. A., Peric, D., & Owen, D. R. (2011). Computational methods for plasticity: theory and applications. John Wiley & Sons.

Hieu, P. T., & Tung, H. V. (2019). Thermal buckling and postbuckling of CNT-reinforced composite cylindrical shell surrounded by an elastic medium with tangentially restrained edges. Journal of Thermoplastic Composite Materials, 0892705719853611.

Kant, T. (1992). A general fibre-reinforced composite shell element based on a refined shear deformation theory. Computers & Structures, 42(3), 381-388.

Librescu, L., & Lin, W. (1997). Vibration of thermomechanically loaded flat and curved panels taking into account geometric imperfections and tangential edge restraints. International journal of solids and structures, 34(17), 2161-2181.

Panda, S. K., & Singh, B. N. (2009). Thermal post-buckling behaviour of laminated composite cylindrical/hyperboloid shallow shell panel using nonlinear finite element method. Composite Structures, 91(3), 366-374.

Pawsey, S. F., & Clough, R. W. (1971). Improved numerical integration of thick shell finite elements. International journal for numerical methods in engineering, 3(4), 575-586.

Ram, K. S., & Babu, T. S. (2002). Buckling of laminated composite shells under transverse load. Composite structures, 55(2), 157-168.

Singha, M. K., Ramachandra, L. S., & Bandyopadhyay, J. N. (2006). Nonlinear response of laminated cylindrical shell panels subjected to thermomechanical loads. Journal of engineering mechanics, 132(10), 1088-1095.

Sit, M., & Ray, C. (2019). A third order nonlinear model to study the dynamic behaviour of composite laminated structures under thermal effect with experimental verification. Composite Structures, 212, 106-117.

Sze, K. Y., Liu, X. H., & Lo, S. H. (2004). Popular benchmark problems for geometric nonlinear analysis of shells. Finite elements in analysis and design, 40(11), 1551-1569.

Trang, L. T. N., & Van Tung, H. (2018). Nonlinear stability of CNT-reinforced composite cylindrical panels with elastically restrained straight edges under combined thermomechanical loading conditions. Journal of Thermoplastic Composite Materials, 0892705718805134.

Van Tung, H. (2013). Postbuckling behavior of functionally graded cylindrical panels with tangential edge constraints and resting on elastic foundations. Composite Structures, 100, 532-541.

Zhou, Y., Stanciulescu, I., Eason, T., & Spottswood, M. (2015). Nonlinear elastic buckling and postbuckling analysis of cylindrical panels. Finite Elements in Analysis and Design, 96, 41-50.